Enzymatic Activity and Excited State Processes in Protochlorophyllide Oxidoreductase

Sytina, O.

2010

~ CHAPTER 7 ~

Modeling of Multi-Exciton Transient Absorption Spectra of Protochlorophyllide Aggregates in Aqueous Solution

Olga A.Sytina, Vladimir I. Novoderezhkin, Rienk van Grondelle and Marie Louise Groot

Protochlorophyllide (Pchlide) is a natural porphyrin, a precursor of chlorophyll, synthesized by plants for its photosynthetic apparatus. The pigment spontaneously forms aggregates when dissolved in neat water solution. We present here calculations of the transient absorption spectra and its comprising components (ground state bleach, stimulated emission and excited state absorption) for a strongly excitonically coupled linear chain of four Pchlide chromophores, using exciton theory with phenomenological Gaussian lineshapes and without energetic disorder. A refined multi-exciton model which includes static disorder is applied to fit the experimental power-dependent transient absorption spectra of aqueous protochlorophyllide and the kinetics for delay times up to 20 ps after photoexcitation. We show that population up to the 4-exciton manifold is sufficient to explain the pronounced saturation of the bleaching and the shape changes in the instantaneous, t=0.2 ps transient spectra when the pulse energy is increased from 10 nJ to 430 nJ per pulse. The decay of the multi-exciton manifold is relatively slow, and is preceded by a spectroscopically distinct process. We suggest that the exciton states in the Pchlide aggregates are mixed with charge-transfer states (CTS), and that the population and repopulation of the CTS coupled to the exciton states explains the relatively slow decay of the multi-exciton manifold. The relevance of our results to the optical properties and dynamics of natural photosynthetic complexes and the possible physical origin of CTS formation are discussed.

7.1. Introduction

The optical properties of molecular aggregates, which are essentially different from the properties of individual molecules, are based on the collective nature of electronic quantum states. In natural photosynthesis, the light-harvesting optical properties are due to molecular aggregates, protein-pigment complexes[152-156]. The main photochemical processes in light-harvesting complexes are carried out via the involvement of a number of porphyrin-like molecules such as chlorophylls, bacteriochlorophylls and pheophytins. The exciton concept is considered to be the basic idea for describing excitation dynamics in the photosynthetic apparatus[118, 147, 157-162]. Exciton theory also has been successfully applied to describe optical properties of other nanoscale systems, for example conjugated polymers, carbon nanotubes and quantum dots[163].

In this work we apply exciton theory to explain the transient absorption (TA) dynamics of Protochlorophyllide (Pchlide) in aqueous solution. Pchlide is a natural porphyrin, a precursor of chlorophyll a (Chl a) that is synthesized by plants for its photosynthetic apparatus. Pchlide, as has been shown in chapter 6, spontaneously forms aggregates in aqueous solution, similarly to Chl[95]. Close coupling between chromophores leads to an excitonic interaction, which significantly alters their optical properties if compared to the monomer state. The visible absorption spectrum of aqueous Pchlide is characterized by a significant broadening and red shift (figure 7.1), and the excited state displays a fast loss of emission over sub- to ps time ranges (figure 7.2, and figure 6.4 in chapter 6). The amplitude of the bleaching observed in transient absorption displays a pronounced excitation power-dependent saturation effect. Kinetic modeling of the visible TA data, presented in chapter 6, allowed us to disentangle spectra and dynamics typical for low and high excitation powers. We showed that the population of the multi-exciton manifold at high excitation density is characterized by a blue-shifted stimulated emission and red-shifted excited state absorption in comparison to those of the 1-exciton manifold. The relaxation from the multi-exciton into the 1-exciton manifold was shown to proceed with a rate of $(10\ \text{ps})^{-1}$ (chapter 6).

Previously, 1-exciton and 2-exciton states have been experimentally observed in J-aggregates of cyanine dyes (TDBC, TTBC, PIC-Br)[164, 165]. By J-aggregates assemblies of dyes of different morphologies in solution or at solid-liquid interface, are indicated, which in the simplest situation form end-to-end stacked structures. The optical properties of linear and tubular J-aggregates, including of the 1- and 2-exciton states have been studied experimentally and theoretically by Knoester and co-workers[166]. For photosynthetic complexes, there are a few reports of 1- and 2-exciton spectra of LH1/LH2 bacterial antennas[167] and of the major light-harvesting complex LHCII of higher plants[168].

Recently 1- and 2-exciton states in FMO and B820-800 light-harvesting complexes have been studied by 2D photon echo spectroscopy[169, 170]. For hydrated chlorophyll, a calculation of the 1-exciton transition was reported by Linnanto *et al* [129]. Higher exciton states can contribute to transient absorption signals under high excitation intensities, but a theoretical analysis with identification of these states and a quantitative explanation of the corresponding spectral responses has never been performed so far.

This chapter is devoted to the calculation of TA spectra of a strongly excitonically coupled linear chain of four chromophores, using exciton theory. The multi-exciton model includes 1-, 2-, 3-, and 4-exciton bands, with phenomenological Gaussian line shapes and static disorder. We show that multi-exciton manifolds in Pchlide aggregate are created upon absorption of more than one light quantum per aggregate. An aggregate size of four coupled Pchlides is in our case sufficient to explain the pronounced saturation of the bleaching at high pulse energy. Using this model, and accounting for the effects of exciton-exciton annihilation (EEA), we can fit the experimental TA spectra of aqueous Pchlide at delay times up to 20 ps after photoexcitation.

We discuss the possibility that the exciton states in Pchlide aggregates are mixed with charge-transfer states (CTS). The same phenomenon has been proposed to occur in natural light-harvesting systems[171], with clear experimental evidence becoming available later from Stark spectroscopy measurements on LHCa4 complex of plant photosystem I [147] and the PS II RC[172]. Our results in aqueous Pchlide serve as an excellent and simple model system to provide theoretical insight into the mechanism of such mixing.

7.2. Theoretical approach

A Pchlide aggregate is modeled by a linear chain of N molecules (in the numerical examples below we suppose N=4), in a head-to-tail orientation. Absorption of one photon promotes an aggregate into the 1-exciton state (consisting of N exciton sub-levels), absorption of a second photon by the same aggregate promotes it to the 2-exciton state (consisting of N(N−1)/2 exciton sub-levels determined by a superposition of N(N−1)/2 pairs of monomeric excitations), and so on. The maximal number of excitations that can be absorbed is equal to N. The highest, N-exciton state consists of a single sub-level, corresponding to N excitations of N monomers in the aggregate. As a result, for N=4, we obtain four 1-exciton sub-levels, six 2-exciton sub-levels, four 3-exciton sub-levels, and one 4-exciton sub-level.

In the TA experiment population of the excited state proceeds via excitation of the S2 (Soret) band, that is followed by quick relaxation to the S1 band, which is in fact a manifold of 1-exciton states determined by the coherent superposition of the Q_Y transitions

of individual Pchlide monomers. Both S2→S1 internal conversion and equilibration (exciton relaxation) within the S1 manifold are supposed to be fast compared with the time scale of the TA dynamics (which is dominated by 0.5-0.6 ps and 5-10 ps components as shown in chapter 6).

Thus, the TA spectra of the 1-exciton state can be calculated assuming a steady-state Boltzmann distribution of populations of the 1-exciton sub-levels. The TA response associated with the 1-exciton manifold consists of the ground state bleaching (GSB), stimulated emission (SE_1) corresponding to transitions from the 1-exciton states to the ground state, and excited-state absorption (ESA_1) due to the transitions from the 1- to 2-exciton state. The explicit expressions can be found elsewhere[173, 174].

Similarly, the TA of the aggregate upon absorption of the second photon (corresponding to population of the 2-exciton manifold) is given by the GSB, SE_2 (corresponding to the 2- to 1-exciton transitions), and ESA_2 (2- to 3-exciton transitions). At higher excitation energies we can reach the 3-exciton and 4-exciton states via absorption of three and four photons, respectively.

The energies of the exciton levels and the dipole moments corresponding to the transitions between them can be obtained by diagonalization of the 1-, 2-, 3-, and 4-exciton Hamiltonians. The multi-exciton Hamiltonians depend on the site energies of the four molecules and the exciton couplings (interaction energies) between them. The construction of the 2-exciton Hamiltonian is described in detail elsewhere[175]. The calculated multi-exciton TA spectra are averaged over random shifts of the site energies, induced by slow conformations of the complex, the so-called energetic disorder or site inhomogeneity.

7.3. Results

7.3.1. Steady-state and transient absorption difference spectra

Absorption spectra of Pchlide dissolved in THF and neat water (D_2O) are depicted in figure 7.1. Using the spectrum of monomer Pchlide in THF and extinction coefficient of ε = 30.1 L/mM · cm at 630 nm [7, 59], we calculated the dipole strength of Pchlide using the expression by Knox and Spring [176]:

$$D = 9.186 \times 10^{-3} \cdot n \cdot \int \frac{\varepsilon(\upsilon)}{\upsilon} \cdot d\upsilon$$

The obtained magnitude of 27.7 debye^2 is very close to the reported dipole strength of chlorophyll, about 30 debye^2 in solvents with similar refractive indices of n ~ 1.4 [176]. Therefore, in our modeling the couplings within the Pchlide aggregate were chosen to be

adjustable parameters, and were varied around the values typical for tightly packed chlorophyll a aggregates[177, 178], i.e. 100-150 cm^{-1}.

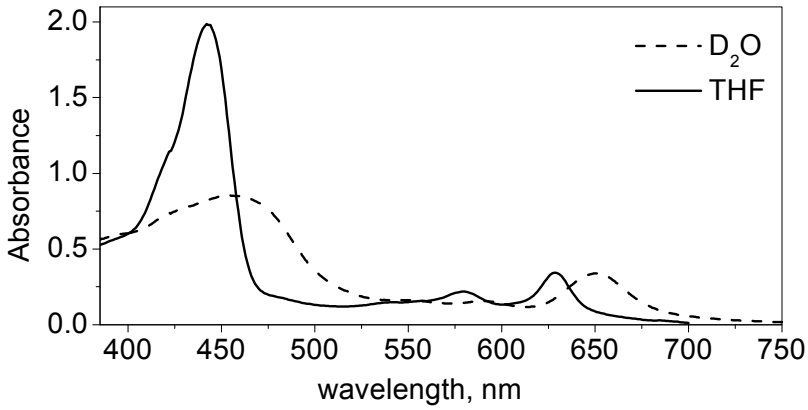

Figure 7.1. Steady-state absorption spectra of Pchlide in THF (solid black line), Pchlide in neat D_2O (dashed black line) recorded in 200mkm cell. The D_2O spectrum is normalized on the maximum of the Q_Y absorption in THF.

In chapter 6 we demonstrated that there is a multi-exponential quenching of the Pchlide excited state signals with rates of about $(0.5\ ps)^{-1}$, $(5\text{-}10\ ps)^{-1}$, $(100\text{-}150\ ps)^{-1}$, and that a long-lived excited state appears, which has a lifetime of about 2.8 ns (see result of global fit of the TA data in figure 6.4). Also, a pronounced power-dependent saturation of the TA signals has been elaborated in more detail. In figure 7.2, we show a selection of the TA spectra demonstrating the relatively fast ($t < 20$ ps) quenching processes at low and high excitation intensities. Immediately after excitation, the 20 nJ and 430 nJ spectra display negative peaks at 659 and 654 nm, respectively, and both signals exhibit a fast decay of these bleachings during the next 20 ps. However, in the 430 nJ case, there is clearly a pronounced decay in the blue wing of the band resulting in an effective red shift of the band's minimum, whereas the 20 nJ spectra show a gradual decay with no spectral shifting at all. Also, the 430 nJ signals are broader and demonstrate different and more complex dynamics than the 20 nJ case and where the 20 nJ spectra are a single band, the 430 nJ spectra appear to be double-peaked.

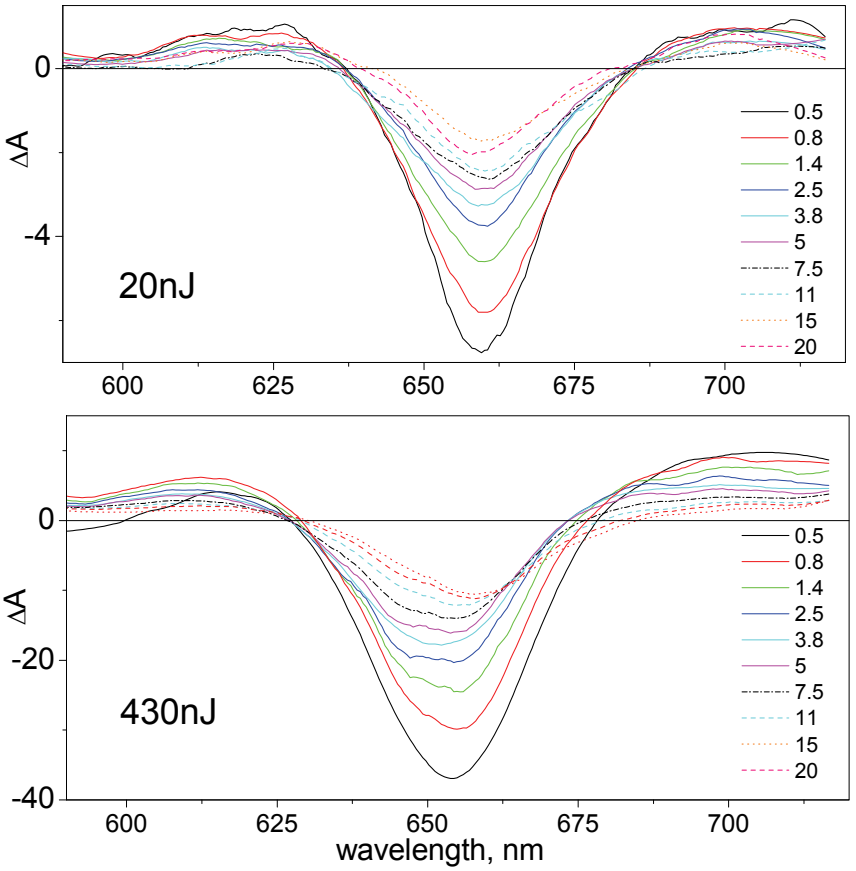

Figure 7.2. Transient absorption spectra measured using pulse excitation energies of 20 nJ (top panel) and 430 nJ (bottom panel), with λexc = 475 nm, at time delays of 0.5, 0.8, 1.4, 2.5, 3.8, 5, 7.5, 11, 15, 20 ps. Note the different scales for the y-axis .

7.3.2. Simulation of TA spectra of linear aggregate

To explain the excitation energy-dependent TA spectra, we use the standard exciton theory as described above in section 7.2. In figure 7.3 we illustrate the structure of the TA spectra corresponding to excitation of 1-, 2-, 3-, and 4-exciton manifolds of a linear chain of N=4 molecules, in a head-to-tail orientation, along-axis orientation of the transition dipoles and with nearest-neighbors couplings of M= –150 cm^{-1}. In this example we do not include

energetic disorder and we use a relatively small homogeneous linewidth, which we assume to be the same for all exciton transitions, in order to highlight the contributions of the GSB, SE and ESA components to the whole TA profile. Population of the sub-levels within each exciton manifold obeys room-temperature Boltzman statistics.

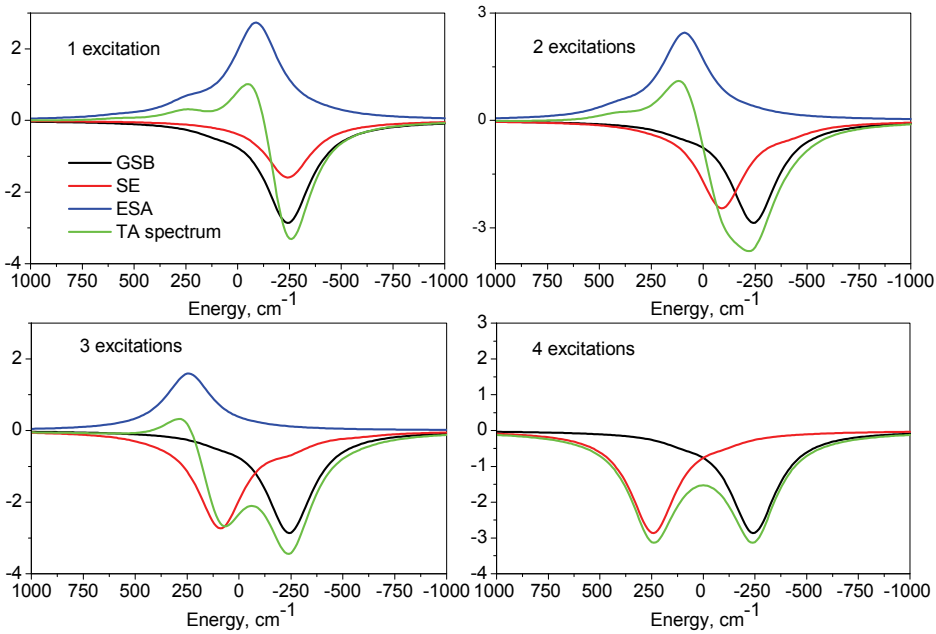

Figure 7.3. Calculated TA spectra and their contributing components as GSB, SE and ESA corresponding to one (A), two (B), three (C), and four (D) excitations of the open linear chain of N=4 identical molecules (head-to-tail orientation, along-axis orientation of the transition dipoles) with nearest-neighbors couplings M=–150 cm^{-1}. Homogeneous width FWHM=250 cm^{-1} is the same for all transitions. Inhomogeneity is not included. The x-scale corresponds to wavenumbers counted from the monomeric transition energy (the same for all 4 molecules) with the energy increasing from the right to the left.

The spectra demonstrate that the GSB component is the same in all cases, but the SE and ESA exhibit a gradual blue shift upon increase in the number of excitations. For one excitation, the SE is less intense than the bleached absorption signal due to population of forbidden 1-exciton sub-levels (which are higher in energy than the superradiant lowest level). For two and three excitations, the SE intensity is increased reflecting an increase in

emitting strength of the lowest 2- and 3-exciton levels. Finally, with four excitations, the SE originating from a single 4-exciton level becomes as intense as the bleached absorption signal. In contrast to the SE, the ESA gradually decreases in intensity and disappears completely in the 4-exciton spectrum, when all the molecules of the aggregate are excited, so that no more excitation is possible. As a consequence, at high excitation density the negative TA peak becomes broader, its center of gravity shifts to the blue, and the integrated intensity (GSB+SE–ESA) increases from 2 (for one excitation) to 8 (for 4 excitations), in units of monomeric dipole strengths. These key properties of the multi-exciton spectra resemble the main features of the experimentally observed spectra, i.e. broadening, blue-shifting/blue shoulder, and increase in amplitude upon increase of the excitation energy (see figure 7.2.)

Hence, we suppose, that the blue shoulder observed in the TA spectra obtained at high energies is related to the population of many-exciton manifolds, whereas the decay of this high-energy TA signal to the normal low-energy spectrum reflects the annihilation dynamics, i.e. relaxation from the many-exciton to the 1-exciton band. The early up to 3.8 ps TA spectra recorded at 20 nJ seem to be indeed comparable with the later, 20 ps spectrum, recorded at 430 nJ in figure 7.2. To further corroborate this hypothesis we performed modeling of the experimental TA spectra at a more quantitative level.

7.3.3. Simulation of real TA data

We start with the fit of the initial TA spectra observed immediately after photoexcitation. In order to fit the data we use a more realistic exciton model that includes disorder. The inhomogeneity is modeled as uncorrelated shifts of the site energies randomly taken from a Gaussian distribution with a FWHM of 100 cm^{-1}. The homogeneous width is increased to 590 cm^{-1} (FWHM), nearest-neighbors couplings are M= –130 cm^{-1}, and a phenomenological Stokes shift for all the SE bands of 100 cm^{-1} is introduced. The unperturbed site energies (identical for all four molecules in the aggregate) are adjusted in such a way to reproduce the GSB at low excitation energy peaking near 659-660 nm. The fit of the initial TA shapes (0.2 ps delay counted from the maximal overlap of pump and probe) is shown in figure 7.4. Figures 7.4.A, B illustrate the broadening and blue shift of measured and calculated spectra corresponding to excitation energies from 20 nJ to 430 nJ, and figure 7.4.C shows the nonlinear effects in the absorption (saturation effect). In order to illustrate the pronounced saturation behavior the TA amplitudes have been normalized to the excitation power.

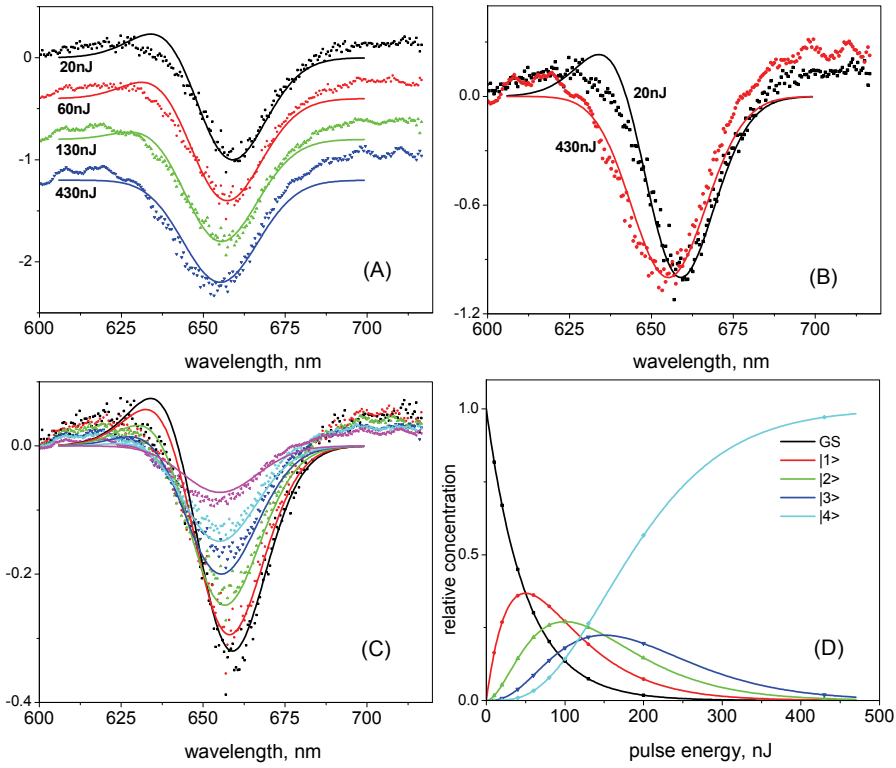

Figure 7. 4. (A). Blue shift and broadening of the measured and calculated TA spectra at different excitation energies, at t=0.2 ps. TA shapes are normalized to unity and shown with vertical offsets of 0.4; **(B)** Comparison of the normalized TA spectra for 20 and 430 nJ. Spectra are the same as in panel (A), but without vertical shift; **(C)** Saturation of the amplitudes of the TA spectra (a.u.) normalized to the excitation energy. Excitation energy is 20 (black), 40 (red), 80 (green), 130 (blue), 200 (cyan), and 430 (magenta) nJ; **(D)** Population of the ground state GS and 1, 2, 3, 4-exciton manifolds plotted as a function of excitation power.

The simplified model in figure 7.3 predicts that the integrated bleach is proportional to the number of absorbed quanta. This implies that without saturation (i.e. when the number of absorbed quanta would be proportional to excitation energy) the normalized bands would have the same amplitudes near 660 nm (with some decrease in amplitude due to broadening). In the more realistic model, at higher excitation energies, progressively

more aggregates have been excited to the 4-exciton state, and it is increasingly more difficult to absorb one more quantum. In the limit of very high energy, all the aggregates are in the 4-exciton state and no further absorption is possible, so that any increase in energy does not increase the TA amplitude. As a result, the normalized TA amplitudes are not constant, but show a dramatic decrease upon increase in excitation energy. The corresponding populations of the 1-, 2-, 3-, and 4-exciton bands as a function of excitation energy are shown in figure 7.4.D.

The described multi-exciton model allows a good fit of the TA shapes and amplitudes within the 20 – 430 nJ range of powers. The TA shapes are well reproduced, including the effects of broadening and blue-shifting at high energies. Some deviations at the blue ($\lambda < 635$ nm) and red ($\lambda > 680$ nm) sides are likely to be related to the simplicity of the model, that limits the aggregate size to four, and neglects variations in its size, and excited state absorption from S1 to S2. Also we used here a phenomenological line shape, without accounting for the phonon-induced effects like vibrational sub-bands, reorganization shifts, relaxation broadening, etc. At the red side the deviation may originate from the contribution of ESA of another, possibly charge-transfer nature, which will be discussed below in more detail.

The saturation behavior is reproduced as well, but the model gives slightly weaker saturation in the 0-200 nJ region and deeper saturation than measured at higher energies. The main source of this discrepancy could be a difference in absorption cross section for the 475 nm pump in the ground and many-exciton states. Depending on the exciton structure of the Soret band and overlap of the pump spectrum with the excited-state Soret transitions (features that are beyond the limits of our current model) one can find different scenarios, like an increase or decrease in effective absorption cross section vs the number of excitations. In figure 7.4 we use the simplest model where the cross section is supposed to be constant. Supposing some decrease of its value for the 2-, 3-, and 4-exciton bands, the fit of the experimental saturation curve can be improved.

7.3.4. Simulation of TA decay dynamics

In this section we focus on modeling of the TA dynamics. The excited state of Pchlide in aqueous solution demonstrates a multi-exponential decay of TA signal on relatively fast sub-ps and ps timescales, and slower ~100 ps timescale. However, here the model is restricted only to the initial 20 ps dynamics, where time constants of 0.5 ps and 2-10 ps were resolved in the global analysis of the TA signal (chapter 6).

It is clearly seen from the experimental data that a two-fold decrease of the TA signal occurs in the fast phase (compare 0.5 and 3.8 ps spectra in figure 7.2). However this

decrease cannot be related to annihilation behavior because (i) the two-fold decrease occurs both for low and high excitation energies, and (ii) the decrease is not accompanied by a red shift typical for an annihilation process. Therefore it is unlikely that this process is dominated by exciton-exciton annihilation. Alternatively, it can be assigned to a relaxation to some dark states, thereby loosing a significant amount of SE signals. Most probably, such a dark non-fluorescent state is a charge-transfer state (CTS), which can be intrinsically facilitated by the structure of the aggregate.

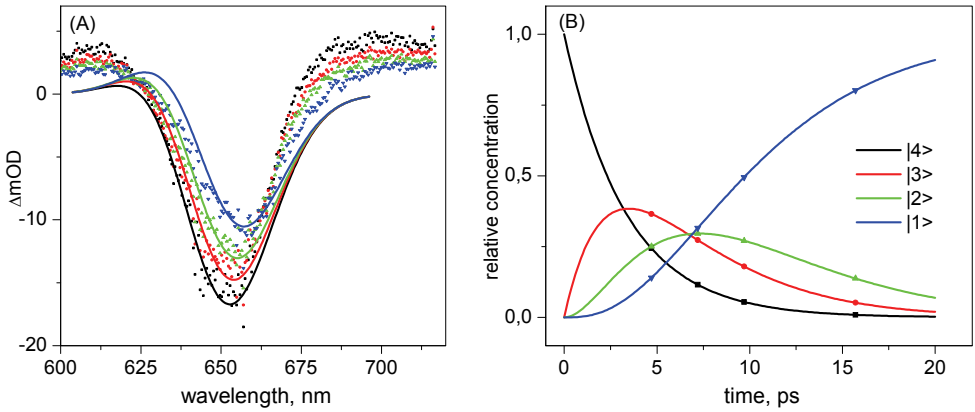

Figure 7.5. Modeling of slow TA dynamics. **(A)** Measured and calculated TA spectra upon 430 nJ excitation for delays t=5, 7.5, 10, and 16 ps. The monomeric transitions are supposed to be 3 nm blue-shifted in order to account for a partial quenching of the stimulated emission during the fast phase. **(B)** Dynamics of the populations of the 4- 3- 2-exciton bands (black, red, green) annihilating to the 1-exciton manifold (blue) plotted as a function of time.

According to the calculated TA spectra in figure 7.3, the transition from the 4,3,2,-exciton states to the CT state should result in loss of blue emission, and the transition from the 1-exciton state in the loss of red emission. This complex situation is very well resolved in the target analysis (chapter 6, figure 6.6.A). Here we can see that the blue emission of the multi-exciton manifold is quenched about a factor of two, and more so at the relatively red side of this emission, on the 0.7 ps time scale. To further complicate the situation, S2 to S1 relaxation and vibrational cooling were shown in monomer Pchlide to occur on this time scale and to give rise to a blue shift of transient absorption signals due to the combined blue shift of SE and ESA (elaborated in chapter 5).

The fast dynamics is followed by a slower phase, displaying the characteristic feature of excitation energy annihilation, i.e. the TA bleach decays together with its red-shifting, clearly resolved at high excitation energies (figure 7.2 compare 5-20 ps spectra in the 430 nJ panel). The TA shape transformation during this slow phase can be reproduced satisfactory by the model, by including a cascading annihilation from 4-, 3-, and 2-exciton bands with a phenomenological rate constant of 0.25 ps^{-1} (4 ps) (figure 7.5). Here, since it is difficult to determine quantitatively the contributions of the effects described above, associated with the transition to the CT state, and vibrational cooling, the overall blue shift of the TA spectra was modeled phenomenologically by shifting the monomeric transitions by 3 nm to the blue from its typical position (figure 7.5). Notice that the positive TA signals measured at wavelengths longer than 680 nm most probably reflect some non-excitonic features, probably excited state absorption from the dark charge-transfer states formed in the first few picoseconds.

7.4. Discussion and Conclusions

In this work we provided a concise description of the spectroscopic data of Pchlide in aqueous solution in terms of exciton theory. First we presented an illustrative example of calculated TA spectra of a linear aggregate with multiple excitations, showing the GSB, SE and ESA contributions. For the simulation of the real TA data we showed that (i) the TA spectra and the dynamics up to 20 ps of Pchlide in water are well described by a rather simple model with phenomenological line shape and static disorder; (ii) the characteristic features of the multi-exciton manifolds are necessary to describe the change of the TA spectra as the excitation power is increased; (iii) however, the red ESA and the initial decay and blue shift of the signal cannot be described by exciton theory, and are most likely due to a coupling of the exciton manifolds to charge-transfer states, combined with S2 to S1 relaxation and vibrational cooling.

7.4.1. Energy level scheme in Pchlide aggregate

Based on our results, we can now construct an energy level scheme of the Pchlide aggregates, that includes the description of the excited state as a number of collective (exciton) states, determined by a coherent superposition of the individual (monomeric) excitations, and the phenomenological coupling of each exciton state to a CT state see (figure 7.6). Excitation of the S2 (Soret) exciton band by a 475 nm laser pulse is followed by a partially rapid (100-200 fs) and partially slower (0.5 ps) radiationless transition from the S2 to S1 (Q_Y) exciton state and fast (<100 fs) equilibration within the exciton sub-levels

of the Q_Y band. At high excitation energy, the 2-, 3-, or 4-exciton Q_Y manifolds are populated by the same mechanism. A subsequent decay of these multi-exciton states occurs via a reversible transition to dark CT states, and via step-by-step cascading down to the lowest 1-exciton state due to exciton-exciton annihilation processes.

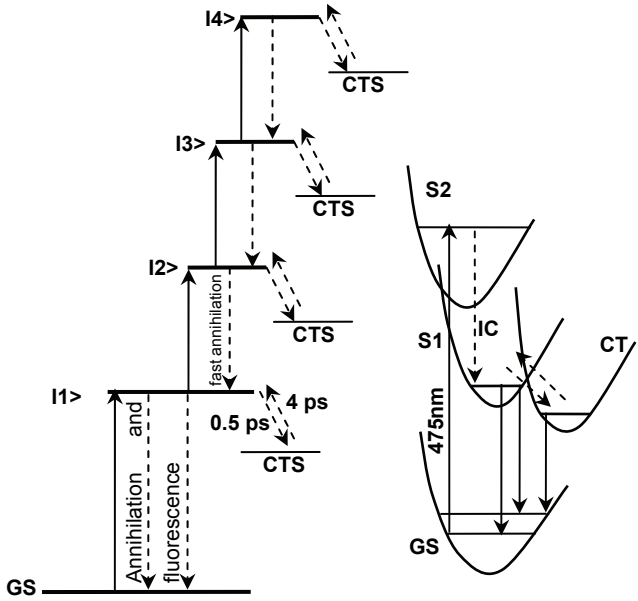

Figure 7.6. Energy level diagram and multi-exciton dynamics in Pchlide aggregate. In the scheme promotion to the exciton excited states is shown by solid arrows, for simplicity the S2 →S1 fast relaxation is neglected. In the right hand panel a more detailed scheme of CT mixing with the S1 exciton state is shown, with the initial population of the S2 state according to experiment. See also figure 6.8 in chapter 6.

7.4.2. Explaining fast and slow dynamics

With a time constant of 0.5 ps (derived from target analysis in chapter 6) relaxation to the CT states occurs and an equilibrium between population of exciton and CT states is achieved. Later, 5-20 ps after excitation, we observe dynamics with spectral signatures typical for annihilation. However this is very slow when compared to annihilation rates expected for a tightly-packed aggregate[129, 139]. Most probably the rate of the annihilation itself is fast enough, corresponding to the sub-ps time scale, but the effective annihilation is

limited by the slow back transfer from the CT states. The rate of such re-pumping of the multi-exciton manifolds is determined by up-hill transfer over the barrier separating the excited and CT states. Therefore, the observed TA decay is not determined by the pure fast annihilation rate, but by the slow back energy transfers from CTS to the exciton excited states. The phenomenological effective rate of annihilation of the excited state (0.25 ps^{-1} in our model) thus describes the back transfer from the CTS state to the excited state. This population and repopulation of the CTS coupled to exciton states giving rise to delayed annihilation is similar to the delayed fluorescence induced by slow radical pair recombination in photosynthetic reaction centers[179].

7.4.3. Possible physical origin of the CT state in Pchlide aggregate

In this work we interpret the dynamics of the Pchlide excited state in aqueous solution as a sequence of charge separation events combined with exciton-exciton annihilation (EEA) effects. Previously, in chapter 6, we discussed aspects of the possible structural organization of the Pchlide aggregate in water solution. Basically, we suggested that similar to hydrated chlorophylls[122, 123], Pchlide monomers are coordinated via an internal water bridge between Mg atoms and C=O keto groups of adjacent molecules. The loss of signal strength of the Pchlide C=O mode in the excited state in the mid-IR data (figure 6.7) implies that the C=O oscillator strength is significantly reduced, which can be caused by appearance of additional charge on the keto site. Generally speaking, the processes of site-specific solvation or (de)protonation of the keto bond in the excited state can be directly related to formation of a state possessing a charge-transfer character, and facilitated by the acidic character of the coordinating water molecule as compared to bulk water. This resembles the processes of tautomeric proton transfer from the keto to the enol state upon photo excitation of the dimer in chlorophyll water adduct states, discussed by Fong, Shipman, Wasielewski, Katz and others [122, 123, 143]. Basically, the mechanism involves the breaking of the H-bond in the internal coordinating water bridge, leading to ligation of Mg with an OH ion and protonation of the C=O keto group of the other chlorophyll. The process can also be considered as the well known metal–to-ligand (MLCT) / ligand-to-metal charge-transfer (LMCT) state formation [180, 181]. The quenching properties of water and the OH^- ion on fluorescence and lifetime shortening[182] have been observed in many chromophores besides chlorophylls, and is usually associated with protonation, see for example aniline derivatives [183, 184], salicylic anion[185] and organic dyes[186, 187].

7.4.4. Relevance to dynamics in light-harvesting complexes

The resemblance between the observed TA saturation and spectral dynamics in aqueous Pchlide with data from more complicated natural light-harvesting systems such as CP43[132] and CP47[67] in photosystem II (PSII) has already been noted in chapter 6. In CP43/47 complexes, as well as other plant photosynthetic protein complexes such as the reaction centers (RCs) in PSI and PSII, the light-harvesting complex Lhca3-4, LHCII, and also the LH1 and LH2 complexes in photosynthetic bacteria, extremely red-shifted and broadened absorption and emission bands have been detected [67, 132, 147, 171, 188-192]. For example, the 745-760 nm emission wings in PSI from cyanobaterium T.elongatus is up to 90 nm red-shifted from the dominating band at 670 in absorption and 680 nm emission [190].

The origin of these red states was initially attributed to be due to so called red Chls, minor groups of strongly excitonically coupled pigments, which might be a consequence of tight packing inside light-harvesting proteins. However, the excitonic nature of low energy transitions alone can not explain the extreme red shift and broadening of spectra. In J-aggregates excitonic coupling does not result in the broadening of bands, but in a narrowing of the excitonic band[193]. A similar effect was found for light-harvesting photosynthetic complexes[194].

The effect of mixing of the lowest exciton state with the excited charge-transfer state has been proposed in numerous works on natural light-harvesting systems to explain the phenomena of red states and extreme broadening [144, 171, 189], and was confirmed experimentally by applying Stark spectroscopy to Lhca-4 from PSI[147], special pair RC[195], LH1 and LH2 complexes[196, 197]. Also the effect of polaron formation 10 ps after excitation, resulting from coupling between exciton and CT states, has been suggested to explain TA dynamics in the bacterial LH2 complex on time scales up to 100 ps[192, 198]. A polaron, defined as an electronic state accompanied by lattice deformation, leads to strong localization of the exciton state on just a few BChls, between one and four. The progressive red shift in 100 ps of the GSB was associated with solvation/relaxation of the polaron state.

In reaction centers (RC) of PSII the lowest excited state is formed by a coherent superposition of wavefunctions of several pigments (the accessory Chls a, the pheophytins and the special pair of chlorophylls). The coupling of a charge-transfer state with any of the six pigments results in an effective mixing of CT states with the whole set of exciton states. In such a way the process of primary charge separation can be effectively directed towards the most favorable pathway, which depends on the particular realization of disorder, i.e. conformational state of RC[171]. According to results obtained from applying modified Redfield theory to model the absorption and transient absorption changes in the PSII RC,

the coupled CT state is multi-exponentially populated with the rates between (100 - 500 fs)$^{-1}$ [199] , which is very similar to our estimates for the Pchlide aggregates.

As mentioned in section 7.4.3, the H-bonding interaction is likely to be an important (if not decisive) factor for formation of the CTS in Pchlide aggregates, and therefore should be considered as an important factor in explaining the extreme broadening. In our model, the total width of the one-exciton absorption determined mostly by the lowest transition is about 700 cm^{-1}. It is likely that in aqueous Pchlide a variable and dynamic coordination interaction strength inside the aggregate and with the bulk water network, is responsible for the significant total homogeneous and inhomogeneous broadening of the Q_Y absorption band, and also facilitates mixing of the exciton states with CT.

The presence of a strong H-bonding interaction with the surrounding protein residues has also been demonstrated in the CP47 complex by FLN spectroscopy[191]. The vibrational frequency of the keto C=O mode associated with the red states in CP47 complex were found to be extremely downshifted to 1633 cm^{-1} with respect to the usual position at 1686-1664 cm^{-1} in monomer/or weakly coupled pigments[67]. In aqueous ethanol solution of zeaxanthin, pH, and consequently, the ability to form H-bonds was shown to be crucial for formation of H-aggregates[200].

These examples and our own results on aqueous Pchlide reflect that CTS mixing with exciton states is a common and intrinsic phenomenon in natural photosynthesis, determined by not only mutual organization of the pigments but also facilitated by H-bonding interactions. We believe that the current results, presented here and in chapter 6, will contribute to a better understanding of the complex dynamics observed in natural photosynthetic systems.